Am J Transl Res 2021;13(1):270-285
www.ajtr.org /ISSN:1943-8141/AJTR0114955

Original Article

Inhibition of mTORC1 in the rat condyle subchondral bone aggravates osteoarthritis induced by the overly forward extension of the mandible

Yazhen Li[1,2*], Jing Yang[3*], Ying Liu[4], Xiao Yan[1], Qi Zhang[1], Junbo Chen[1], Qiang Zhang[1], Xiao Yuan[1]

[1]Department of Orthodontics, The Affiliated Hospital of Qingdao University, Qingdao, Shandong, China; [2]State Key Laboratory of Oral Diseases, National Clinical Research Center for Oral Diseases, West China Hospital of Stomatology, Sichuan University, Chengdu, Sichuan, China; [3]Qingdao Stomatological Hospital, Qingdao, Shandong, China; [4]Department of Stomatology, Secondary Hospital of Shandong University, Jinan, Shandong, China. [*]Equal contributors.

Received May 25, 2020; Accepted November 11, 2020; Epub January 15, 2021; Published January 30, 2021

Abstract: The present study aimed to investigate the role of mammalian target of rapamycin complex 1 (mTORC1) in the remodeling of the condyle subchondral bone in rats with temporomandibular joint osteoarthritis (TMJ OA) and explore the mechanisms involved. In this study, we used rats fitted with appliances to overly extend the mandible forward as an animal model of TMJ OA. Bone samples were collected 2, 4, and 8 weeks after appliance fixation. Histological changes in the condyle subchondral bone were assessed by staining with hematoxylin and eosin, safranin O, and tartrate-resistant acid phosphatase. Real-time polymerase chain reaction and immunohistochemical analyses were performed to evaluate the expression levels of osterix, runt-related transcription factor 2 (RUNX2), osteocalcin (OCN), and mTORC1 in the condyle subchondral bone. The dissected condyles were analyzed using a micro-CT scanner. We also investigated changes in the condyle subchondral bone after mTORC1 pathway inhibition. In the early stages of TMJ OA, preosteoblasts, osteoblasts, and osteoclasts of the condyle subchondral bone were activated, which stimulated subchondral bone loss. MTORC1 was activated in subchondral bone preosteoblasts in rats with TMJ OA. The mTORC1 pathway was inhibited by a local injection of rapamycin, and the number of osteoblasts and mRNA levels of osteogenic markers in the condyle subchondral bone decreased, but the number of osteoclasts was basically unchanged. As a result, in the early stages of TMJ OA, subchondral bone loss and aggravation of OA were observed. These findings suggest that the mTORC1 signaling pathway plays an important role in subchondral bone remodeling during early stages of TMJ OA.

Keywords: Temporomandibular joint, osteoarthritis, mTORC1, subchondral bone

Introduction

Temporomandibular joint osteoarthritis (TMJ OA) is a progressive, degenerative disease that gradually affects the cartilage, synovial membrane, and bony structures. Chondrocyte death, cartilage matrix degradation, early stage subchondral bone resorption, and advanced-stage subchondral bone sclerosis are frequently reported in TMJ OA [1]. Clinically, TMJ OA mainly manifests as joint pain, murmur, friction, or popping; restricted mouth opening; abnormal jaw movement; maxillofacial deformity; and partial opening and closing [2]. Therefore, TMJ OA not only affects the health of the patient's oral and maxillofacial system, but may also cause psychological impairment [3].

The TMJ is one of the most common sites of OA, which has a large impact on joint function. The risk factors for TMJ OA are complex and related to both mechanical injury to and inflammation of the joint. Excessive mechanical stress on the TMJ, such as severe malocclusion, is considered one of the main causes of TMJ OA [4-6]. Overloading the TMJ is usually thought to initiate the destruction of the cartilage matrix, leading to OA [4]. Loss of posterior teeth, experimental posterior teeth occlusal disorder, and unilateral anterior crossbite prostheses have been shown to cause TMJ OA-like lesions or significant TMJ degradation [7-9]. Similarly, excessive mandibular protrusion may also cause OA-like symptoms.

The pathogenesis of TMJ OA is still unclear, yet the involvement of subchondral bone tissue during the development of OA is likely [10, 11]. In recent years, researchers have paid increased attention to the inflammation and remodeling of subchondral bone in the early stages of TMJ OA. Studies have shown that subchondral bone undergoes resorption during early OA and sclerosis during advanced OA [12-14]. Most notably, structural changes in the subchondral bone have an important impact on the degeneration of the articular cartilage [15-17]. Studies on the condyle subchondral bone may clarify the pathological mechanism of TMJ OA.

The mammalian target of rapamycin (mTOR), which regulates cell growth, proliferation, and metabolism, is a protein kinase found in mTOR complex 1 (mTORC1) and mTOR complex 2 (mTORC2) [18-20]. In mammals, mTOR mainly regulates cellular functions via mTORC1, which can be inhibited by rapamycin (Rapa) [21]. There is evidence that mTORC1 is essential for maintaining the metabolic homeostasis of chondrocytes, and its activation in articular chondrocytes plays a crucial role in the development of OA. Balanced mTORC1 activity is critical for bone metabolism and development by regulating the proliferation, differentiation, and function of osteoblasts and osteoclasts. However, the role of mTORC1 in condyle subchondral bone remodeling and its underlying mechanism during the pathogenesis of TMJ OA have not yet been reported.

The present study aimed to investigate the role of mTORC1 in condyle subchondral bone remodeling using a rat model of TMJ OA and explore the mechanisms involved.

Materials and methods

Experimental animals

Sprague-Dawley rats (140-160 g; 6 weeks of age) were provided by the animal center of Qingdao University. Animals were cared for according to the institutional guidelines set by the University Ethics Committee. This study also complied with Animal Research: Reporting of In Vivo Experiments guidelines for preclinical animal studies. Rats were randomly divided into an experimental group (Exp) or a sham-operated control group (Con). Each group was equally assigned to three (2, 4, or 8 weeks) subgroups by sample collection time point (n = 9).

Experimental procedure

The rats were anesthetized using an intraperitoneal injection of 40 mg/kg pentobarbital. The experimental rats were fitted with appliances to overly extend the mandible forward. The appliances were carefully bonded with zinc phosphate cement (Shanghai Dental Instrument Factory, Shanghai, China) and checked every two days. The inclined guide plate was oriented 30°-40° to the occlusal plane. With the lower arch incisors biting down on the guide plate, the mandible was extended more than 3 mm (**Figure 1A** and **1B**). Thus, the mandible was extended beyond its normal range. No appliances became detached during the experiment. For the control group, the rats underwent a similar procedure but did not wear any functional appliance.

Tissue preparation

Rats were sacrificed 2, 4, or 8 weeks after the procedure. Since no differences in degradation were observed between the left and right TMJ in the Exp group, the left TMJ tissue blocks from five rats were fixed, decalcified, and embedded in paraffin. Fifteen center and near-center 5-mm-thick sagittal sections of the TMJ blocks were prepared by a professional technician. To exclude selection bias, sections were randomly selected for staining with hematoxylin and eosin (HE), safranin O, and tartrate-resistant acid phosphatase (TRAP); immunohistochemial staining for osterix, runt-related transcription factor 2 (RUNX2), osteocalcin (OCN), and mTORC1 was also performed. The right TMJs from four rats were used for micro-CT analysis. For each group, the condyle subchondral bone of the other nine TMJs (including four left side and five right side TMJs) were obtained and stored at -80°C. Three condyles from five different rats were pooled to create a single sample of subchondral bone for RNA extraction.

Injections of drugs

For the control injection (Con+Rapa) and experimental injection (Exp+Rapa) groups, Rapa (5 mg/kg/d) in dimethyl sulfoxide (DMSO) was injected into the TMJ every day for 8 weeks,

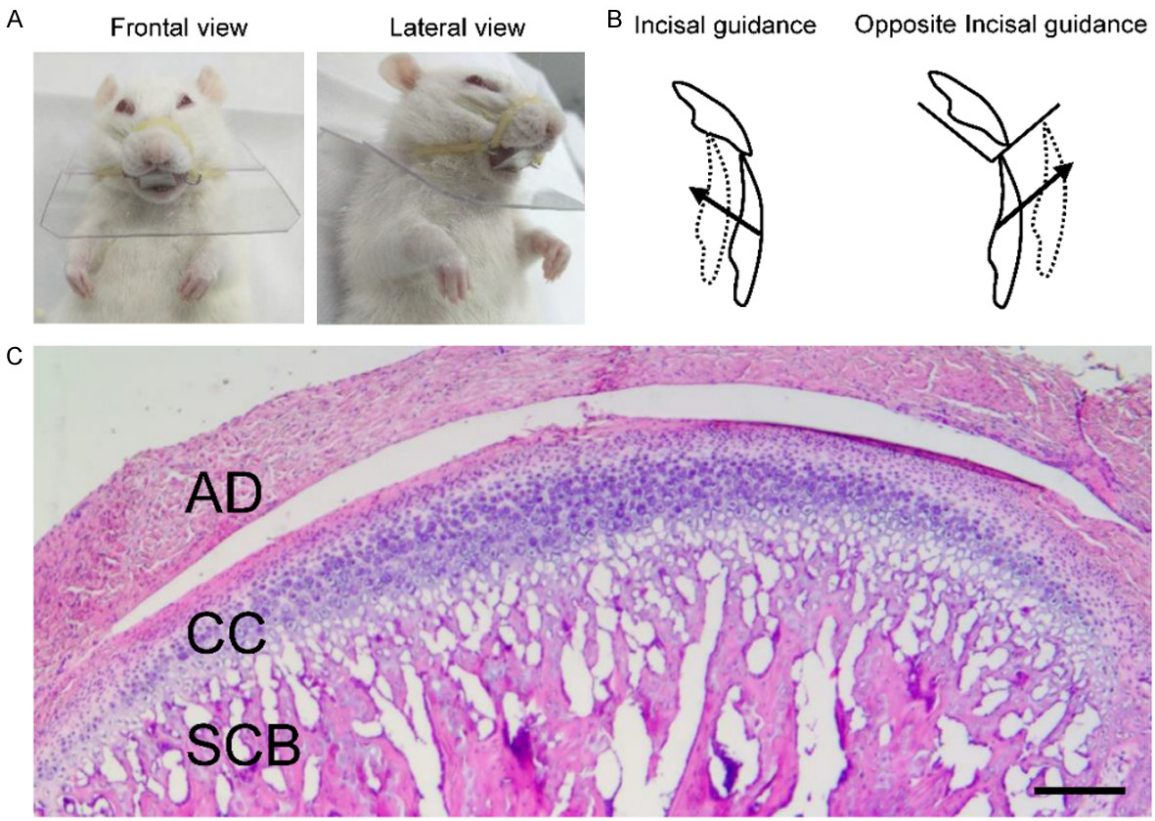

Figure 1. The occlusal relationship of the anterior teeth. A. Representative frontal and lateral views of an experimental rat after the procedure. B. Schematic diagrams of the normal incisal guidance in the control rat and the opposite guidance in the experimental rat when the mandibles are overly extended forward in the sagittal direction during incising. Arrows indicate the direction of the incisal guidance. The bilateral incisors in the control rats provide normal incisal guidance, whereas those in the experimental rats provide incisal guidance in the opposite direction. C. A representative central sagittal HE section of the TMJ from a control rat. AD: articular disc; CC: condylar cartilage; SCB: subchondral bone. Bar = 400 mm.

starting 1 d after model establishment. After the induction of deep anesthesia, rats were positioned on their sides. A custom-made microinjector was inserted at a point just below the zygomatic arch until the outer surface of the mandibular ramus was reached. The orientation of the needle was adjusted so that it could pass along the bony wall and into the TMJ. The drug solution was then injected into the TMJ through the needle. For the control (Con+DMSO) and experimental (Exp+DMSO) groups, the same volume of DMSO was injected into the TMJ.

Histochemical staining and histomorphometry

HE staining was used to assess the histochemical changes in the condyle. Safranin O staining was performed to determine changes in proteoglycans. Briefly, the stained sections were imaged using a Leica DFC490 system (Leica, Wetzlar, Germany). TRAP staining was performed to examine the osteoclast activity of the condyle subchondral bone, following the manufacturer's instructions (Sigma-Aldrich 387-A, St. Louis, MO, USA). TRAP+ osteoclasts were counted in five randomly selected, high-power (400 ×) fields under a microscope (Leica DM 2500), and the average value was used as the value for this section. The number of TRAP+ osteoclasts was averaged from three sections per animal for statistical analyses (n = 5).

RNA extraction and real-time PCR

Total RNA was extracted using the TRIzol reagent (Invitrogen, Carlsbad, CA, USA). The primers for the target genes are listed in **Table 1**. Gene expression was analyzed using an Applied Biosystems 7500 Real-Time PCR machine

Table 1. Gene primers

Genes	Forward Primer	Reverse Primer
Osterix	CTGTGGCAAGAGGTTCACCC	TGATGTTTGCTCAAGTGGTCG
OCN	ATCTATGGCACCACCGTTTA	CCTCATCTGGACTTTATTTTGG
RUNX2	ATGATGGTGTTGACGCTGAT	CAACTGGGGAGTGAATGAGA
TRAP	CACCCGCAACATCTATTACC	CAGCTTCTTCTTGTCAAACTCC
GAPDH	TTCAACGGCACAGTCAAGG	CTCAGCACCAGCATCACC

(Applied Biosystems, Foster City, CA, USA) with glyceraldehyde-3-phosphate dehydrogenase (GAPDH) as the internal control. The results were calculated as the relative quantification compared to the Con group, which was set to 1. Data were collected from three independent pooled samples (n = 3).

Immunohistochemistry (IHC) and immunofluorescence (IF) staining

IHC and IF staining were performed according to the manufacturer's instructions. For IHC staining, the primary antibodies were rabbit anti-osterix (1:100 dilution; Abcam, ab22552), mouse anti-osteocalcin (1:200 dilution; Abcam, ab13418, Cambridge, UK), mouse anti-RUNX2 (1:200 dilution; Santa Cruz, sc-390351, Dallas, TX, USA), and rabbit anti-p-S6 ribosomal protein (Ser235/236; 1:200 dilution; Cell Signaling Technology, #2211, Danvers, MA, USA). For IF staining, secondary antibodies conjugated with fluorescent tags were used, and slides were incubated at room temperature for 1 h in the dark. DAPI was used to stain the nuclei. The data were averaged from three slides per animal. Antibody reactivity was then observed under laser-scanning confocal microscopy (FV1000; Olympus, Shinjuku City, Tokyo, Japan). The number of positive cells was averaged from three sections per animal for statistical analyses (n = 5).

Micro-CT analysis

The dissected mandibular condyles were analyzed using a high resolution micro-CT scanner (Viva CT80; Scanco Medical AG, Bassersdorf, Switzerland). Scanning was performed at 90 kV and 100 μA with a resolution of 10 μm/pixel. The sagittal images of the condyles were used to assess the thickness of the cartilage. In the three-dimensional images, two cubic regions of interest (0.5 × 0.5 × 0.5 mm) at the middle points of the center and posterior condyles were selected to examine the subchondral bone, as previously described [8]. The ratios of bone volume to total volume (BV/TV, %) and bony surface area to bone volume (BS/BV, %), trabecular number (Tb.N), trabecular separation (Tb.Sp), trabecular thickness (Tb.Th), and bone mineral density (BMD) were measured.

Statistical analysis

All results are presented as the mean ± standard deviation using GraphPad Prism, v. 6.00 (GraphPad Software, San Diego, CA, USA) and analyzed using the Student's *t* test or analysis of variance. A *P* value less than 0.05 was considered a significant difference.

Results

Preosteoblasts, osteoblasts, and osteoclasts accumulate in the condyle subchondral bone during early TMJ OA

Samples were taken at 2, 4, and 8 weeks for staining. HE staining showed that the cells in the condylar cartilage of the Con group were arranged in a regular, ordered fashion (**Figure 2A**). Two weeks after the model was established, the cartilage matrix became disordered, which gradually worsened over time. The amount of cartilage matrix proteoglycan decreased, chondrocytes appeared clustered and hypertrophic, and the condyle subchondral bone arrangement became disordered and gradually worsened with time (**Figure 2A** and **2B**). The condylar joints of the Exp group showed mild degeneration at 2 weeks and obvious joint degeneration at 4 and 8 weeks.

Interestingly, the number of osterix+ cells, OCN+ cells, RUNX2+ cells and TRAP+ cells, and the expression of mRNAs in the condyle subchondral bone increased at 4 weeks (**Figure 2C-N**), but resorption of the subchondral condyle was first observed at 2 weeks and peaked at 8 weeks. Results of micro-CT scans further confirmed that BMD, Tb.Th, and BV/TV of the condyle subchondral bone decreased gradually after 2 weeks (**Figure 2O-S**), Tb.N began to decrease at 4 weeks (**Figure 2Q**), and BS/BV and Tb.Sp increased 2 weeks after the model was established (**Figure 2T** and **2U**). The morphology of the condylar bone in the Exp group showed a decrease in trabecular bone density, Tb.Th, Tb.N and BMD. In the early stages of TMJ OA, preosteoblasts, osteoblasts, and osteoclasts of the condyle subchondral bone were

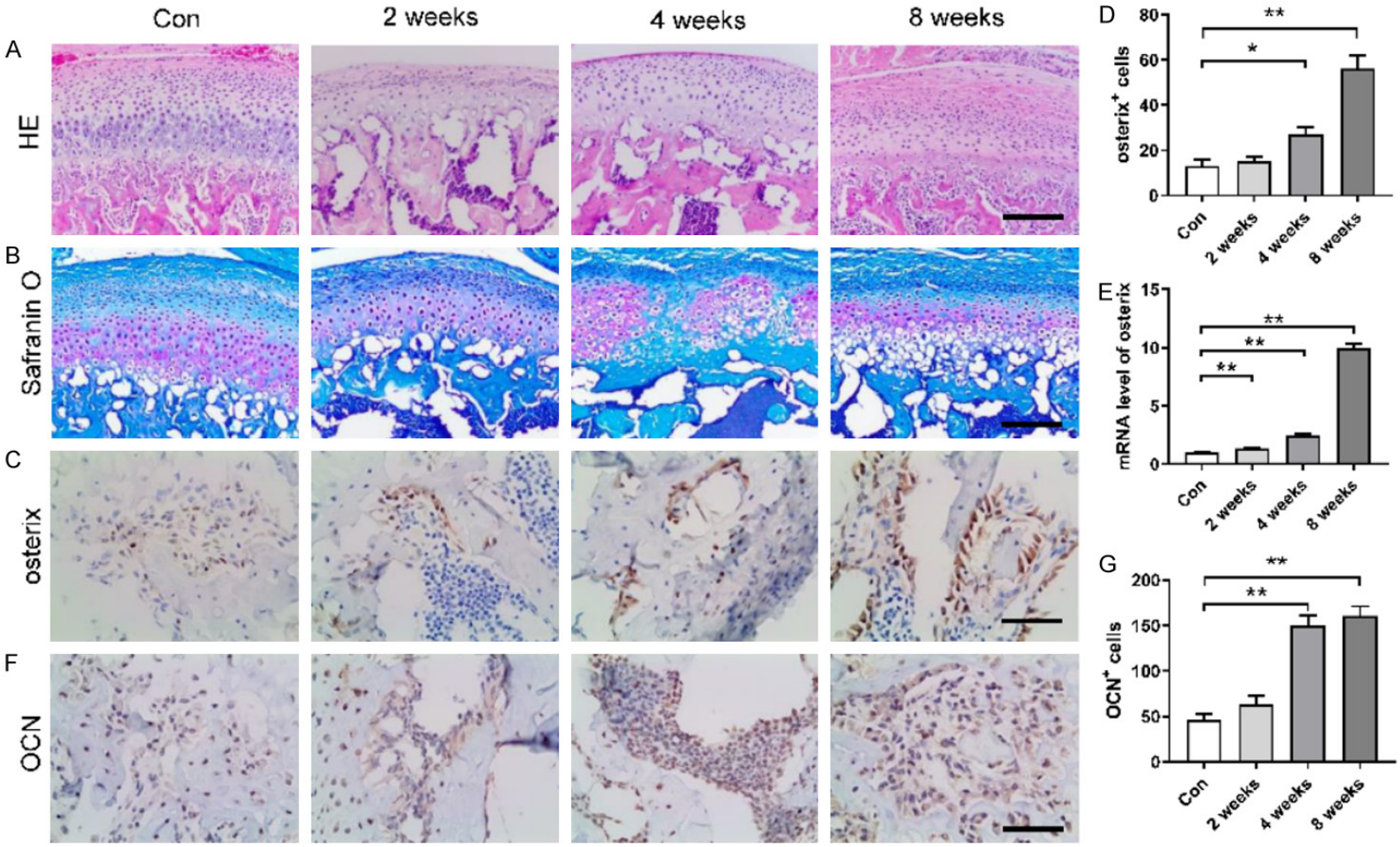
Con
2 weeks
4 weeks
8 weeks
A
HE
B
Safranin O
C
osterix
F
OCN
D
osterix+ cells
E
mRNA level of osterix
G
OCN+ cells

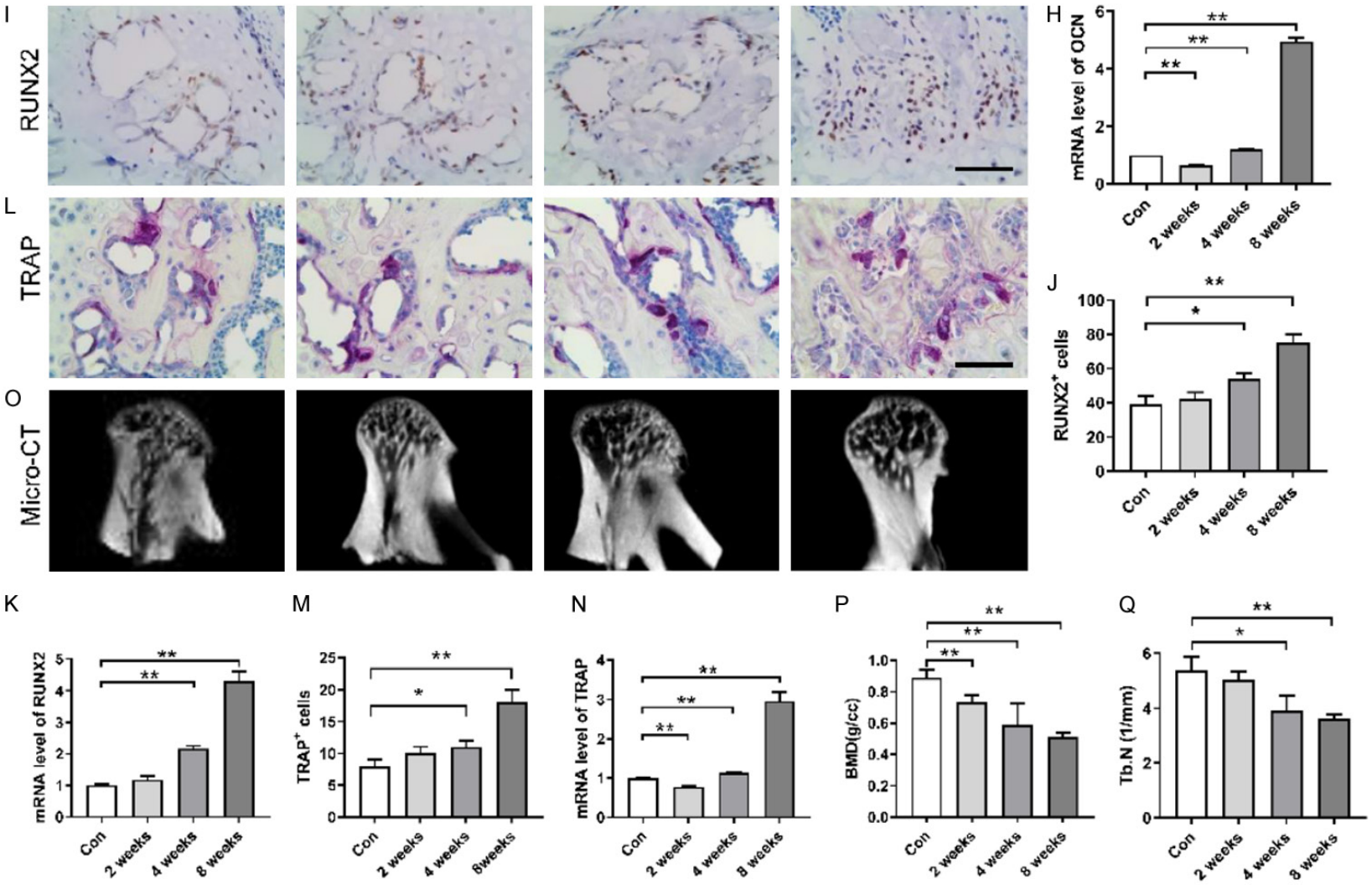
I
RUNX2
L
TRAP
O
Micro-CT
H
mRNA level of OCN
J
RUNX2+ cells
K
mRNA level of RUNX2
M
TRAP+ cells
N
mRNA level of TRAP
P
BMD(g/cc)
Q
Tb.N (1/mm)
Con
2 weeks
4 weeks
8 weeks

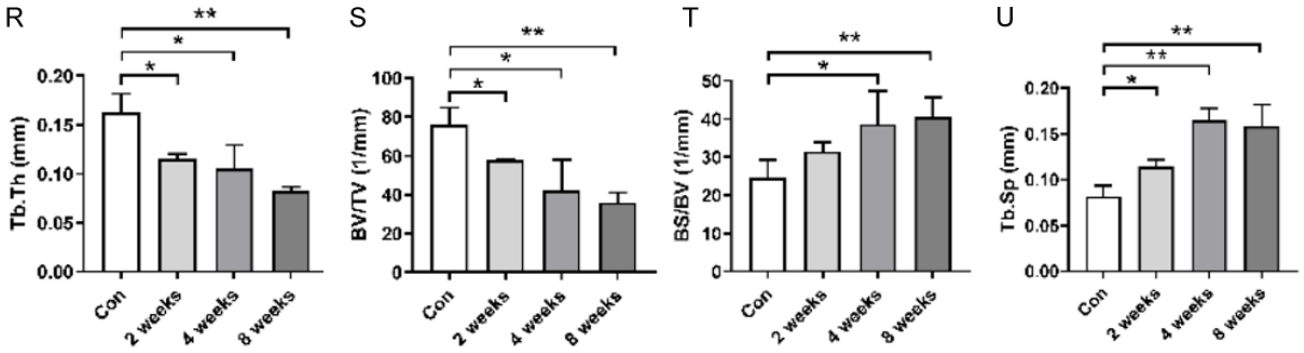

Figure 2. Enhanced osteoclast and osteoblast activities and subchondral bone loss in mandibular condyles. (A and B) Representative HE and safranin O staining, respectively, of sagittal sections of the condyle articular cartilage and subchondral bone in rats with TMJ OA. Scale bars, 200 μm. (C-E) Representative immunohistochemical images (C) and quantitative analyses of osterix+ preosteoblasts (D) and mRNA expression levels of osterix (E) in the condyle subchondral bone at 2, 4, and 8 weeks after the procedure compared with that of the control (Con) group. Scale bars, 50 μm. (F-H) Representative immunohistochemical images (F) and quantitative analyses of OCN+ osteoblasts (G) and mRNA expression levels of OCN (E) in the condyle subchondral bone at 2, 4, and 8 weeks after the procedure compared with that of the control (Con) group. Scale bars, 50 μm. (I-K) Representative immunohistochemical images (I) and quantitative analyses of RUNX2+ osteoblasts (J) and mRNA expression levels of RUNX2 (K) in the condyle subchondral bone at 2, 4, and 8 weeks after the procedure compared with that of the control (Con) group. Scale bars, 50 μm. (L-N) TRAP staining (L) and quantitative analyses of osteoclasts (M) and mRNA expression levels of TRAP (N) in the condyle subchondral bone at 2, 4, and 8 weeks after the procedure compared with that of the Con group. Scale bars, 50 μm. (O) Micro-CT images of sagittal sections and quantitative analysis of the condyle subchondral bone at 2, 4, and 8 weeks after the procedure compared with that of the Con group. (P-U) Quantitative analyses of bone mass in the subchondral bone. (P) BMD (g/cc), bone mineral density; (Q) Tb.N (1/mm), trabecular cell number; (R) Tb.Th (mm), trabecular thickness; (S) BV/TV (%), bone volume fraction; (T) BS/BV (1/mm), bone surface volume fraction; (U) Tb.Sp (mm), trabecular separation. $*P < 0.05$. $**P < 0.01$.

activated, which stimulated subchondral bone loss.

MTORC1 is activated in subchondral mandibular condylar preosteoblasts in rats with TMJ OA

Studies have shown that the pharmacological inhibition or genetic deletion of mTOR in chondrocytes decreases the severity of OA in animal models. When mTORC1 is activated in the subchondral bone at the tibial joint, aberrant subchondral bone formation and secretion of Cxcl12 are induced, accelerating disease progression following surgical destabilization of the joint [22]. However, whether mTORC1 is activated in the condyle subchondral bone and its role in TMJ OA have not been reported. Staining of p-S6 (S235/236, a target and marker of mTORC1 activation) revealed a dramatic increase in the number of p-S6+ cells in the condyle subchondral bones of rats in the Exp group as early as 2 weeks after the procedure (**Figure 3A** and **3B**). Moreover, most p-S6+ cells were located on the condylar surface in rats with TMJ OA. Osterix and p-S6 double-staining confirmed that p-S6 was detected mainly in osterix+ preosteoblasts in the condyle subchondral bones of rats with TMJ OA (**Figure 3C** and **3D**). These results indicate that mTORC1 is activated in condyle subchondral bones, specifically in osteoblastic cells in rats with early TMJ OA.

Inhibition of the mTORC1 pathway in the condyle subchondral bone aggravates subchondral bone loss and the development of OA

To further study the role of mTORC1 activation in TMJ OA, we injected Rapa into the articular cavity to inhibit mTORC1 activation. The condylar tissue was sampled at 2, 4, and 8 weeks. At each time point, the condylar cartilage of the Con+DMSO and Con+Rapa groups presented as a continuous and complete arc, and the cells in each layer of cartilage were well-organized (**Figure 4A**). The condylar cartilage of the Exp+DMSO and Exp+Rapa groups also presented as a continuous and complete arc, but the arrangement of the cartilage layers was disordered, the proliferative layer lacked typical proliferative cells, and the hypertrophic layer was not obvious. Safranin O staining showed that the amount of proteoglycans in the condylar cartilage of the Exp+Rapa group was severely decreased compared to the Exp+DMSO group (**Figure 4B**). The density of the condyle subchondral bone in the Exp+Rapa group was significantly lower than that of the Exp+DMSO group during the same period.

The immunohistochemical staining of p-S6 showed that the number of p-S6+ cells increased in the condyle subchondral bone of the Exp+DMSO group at each time point compared to the Con+DMSO group. The number of p-S6+ cells in the condyle subchondral bone of the Exp+Rapa group decreased after an injection of Rapa. These results suggest that Rapa can inhibit mTORC1 expression in subchondral bone (**Figure 4C** and **4D**).

Immunohistochemical staining and TRAP staining showed that the number of osterix+, OCN+, Runx2+, and TRAP+ cells in the Exp+DMSO group increased significantly compared with the Con+DMSO group, whereas the number of osterix+, OCN+, and RUNX2+ cells in the Exp+Rapa group decreased significantly after an injection of Rapa (**Figure 5A-L**). The osterix, OCN, RUNX2, and TRAP mRNA levels in the condyle subchondral bone displayed the same trend.

These results show that inhibition of mTORC1 signaling pathway decreases the proliferation of subchondral osteoblasts and reduces the osteogenic capacity of the condyle subchondral bone but has little effect on osteoclasts. Micro-CT results confirmed these findings (**Figure 5M-S**). After inhibiting the mTORC1 pathway in the condyle subchondral bone, Tb.Th, Tb.N, and BV/TV decreased; BS/BV and Tb.Sp increased; the BMD of the subchondral bone decreased; and resorption of the subchondral bone became more severe.

Discussion

Current methods for inducing TMJ OA include surgical, spontaneous, and mechanical procedures [8, 9, 23, 24]. Although these approaches can all cause TMJ OA, they also have disadvantages. For example, the genetic mutation model of TMJ OA may cause OA but does not represent a common induction pathway in humans [24]. In addition, inactivated genes may interfere with the normal development of healthy cartilage. For surgical models, contamination of the joint postoperatively and the use of analgesics may interfere with the natural

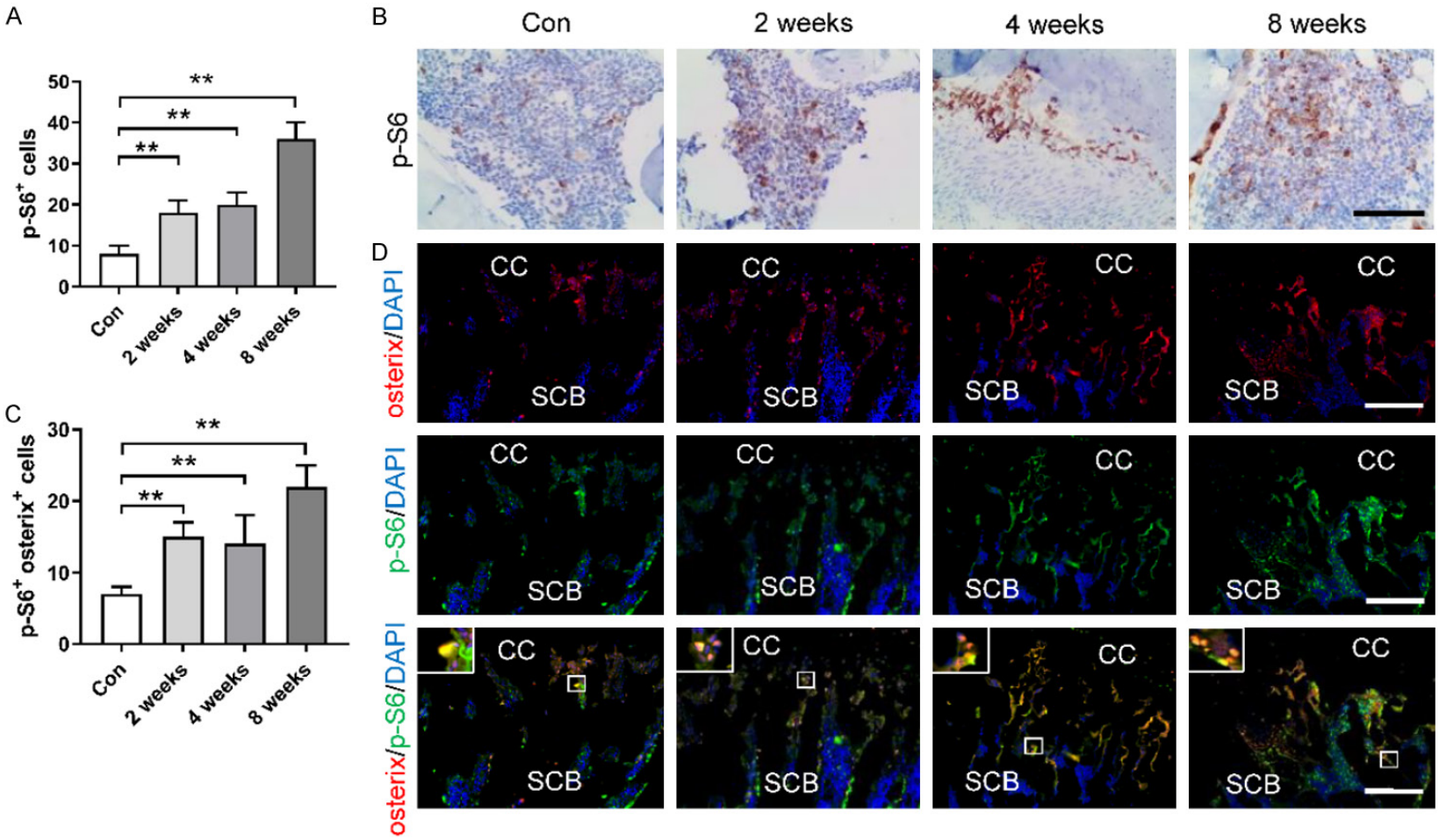

Figure 3. MTORC1 is activated in subchondral mandibular condylar preosteoblasts in rats with TMJ OA. A and B. Representative quantitative analysis and immunostaining, respectively, of p-S6+ cells in the condyle subchondral bones of rats with TMJ OA. Scale bars, 50 μm. C and D. Representative quantitative analysis and immunostaining, respectively, of p-S6 in osterix+ preosteoblasts in the condyle subchondral bones of rats with TMJ OA. The boxed areas in the top left corners are magnified. Scale bars, 200 μm. CC, condylar cartilage; SCB, subchondral bone. *$P < 0.05$. **$P < 0.01$.

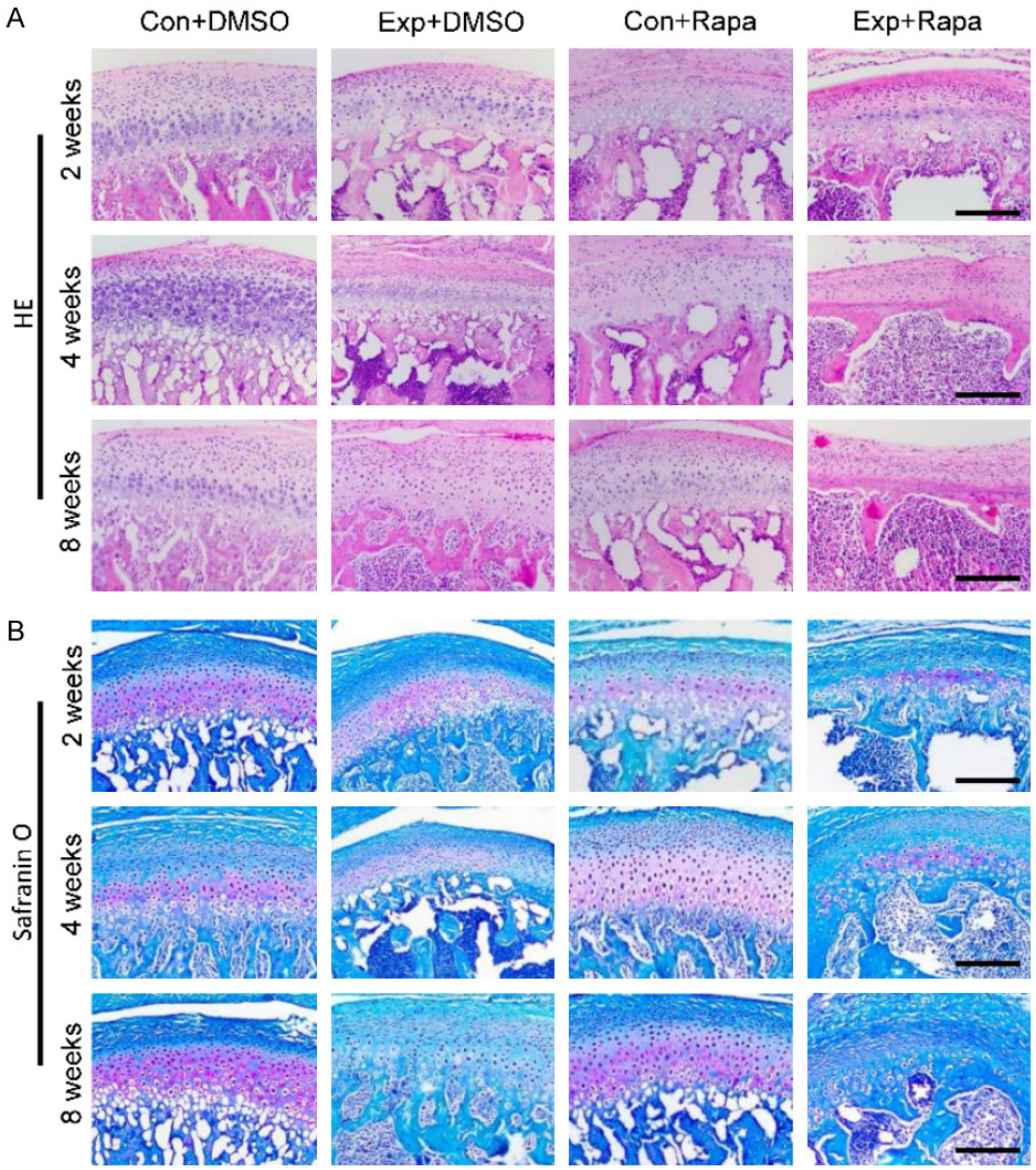
A
Con+DMSO
Exp+DMSO
Con+Rapa
Exp+Rapa
HE
2 weeks
4 weeks
8 weeks
B
Safranin O
2 weeks
4 weeks
8 weeks

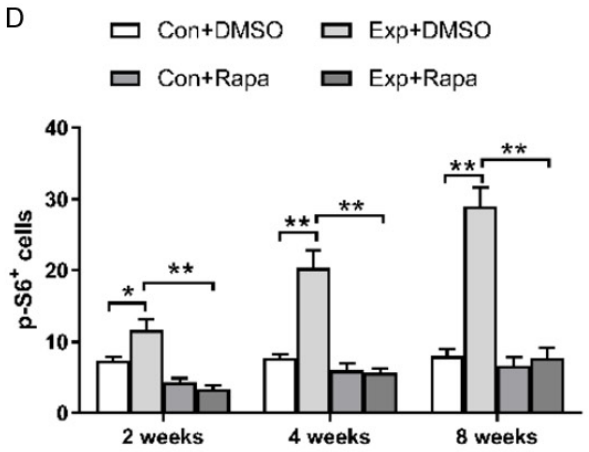
D
Con+DMSO
Exp+DMSO
Con+Rapa
Exp+Rapa
p-S6+ cells
40
30
20
10
0
*
**
**
**
**
**
2 weeks
4 weeks
8 weeks

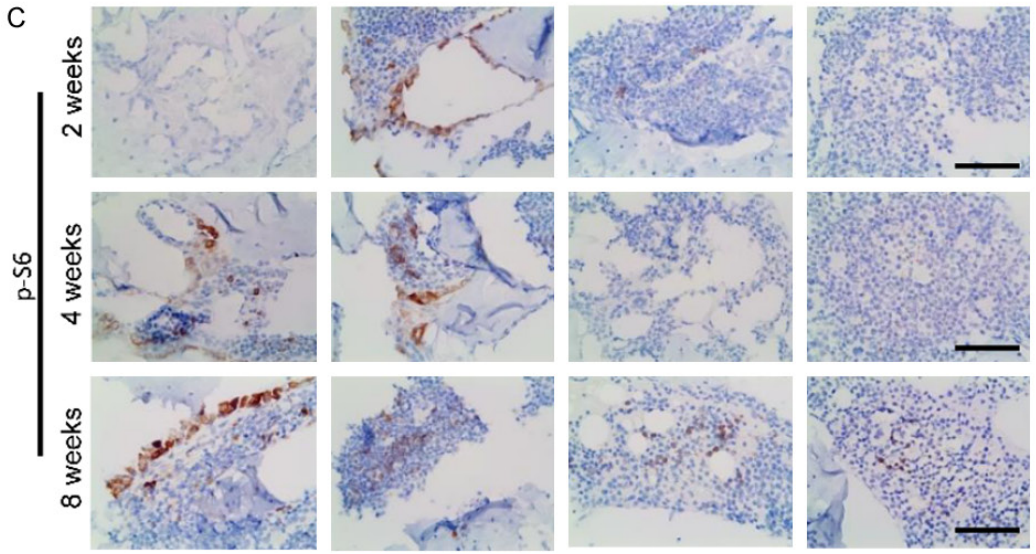

Figure 4. Rapamycin inhibits mTORC1 expression in condyle subchondral bones in rats with TMJ OA. A and B. Representative HE and safranin O staining, respectively, of sagittal sections of condylar cartilage and subchondral bone at 2, 4, and 8 weeks after the procedure in four groups. Scale bars, 200 μm. C and D. Representative immunohistochemically stained images and quantitative analysis, respectively, of p-S6+ cells in the condyle subchondral bone at 2, 4, and 8 weeks after the procedure. Scale bars, 50 μm. *$P < 0.05$. **$P < 0.01$.

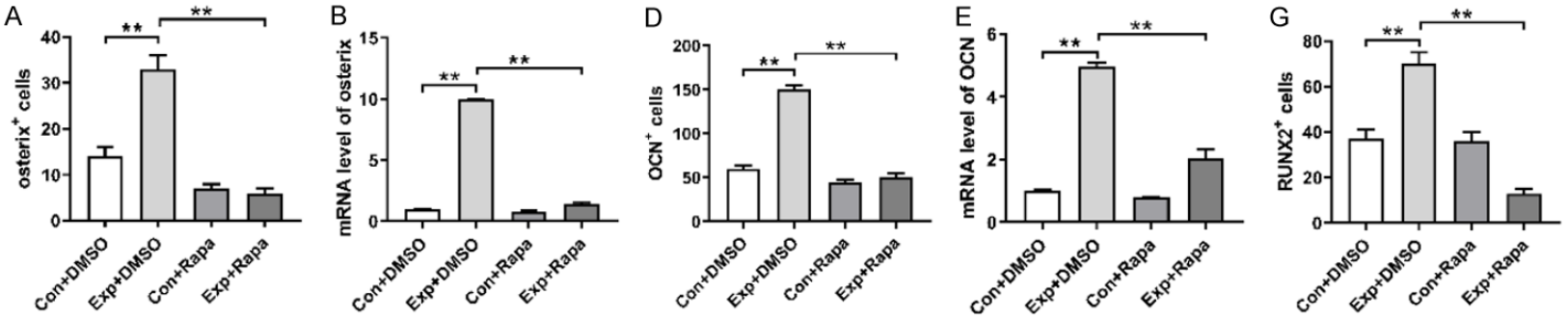

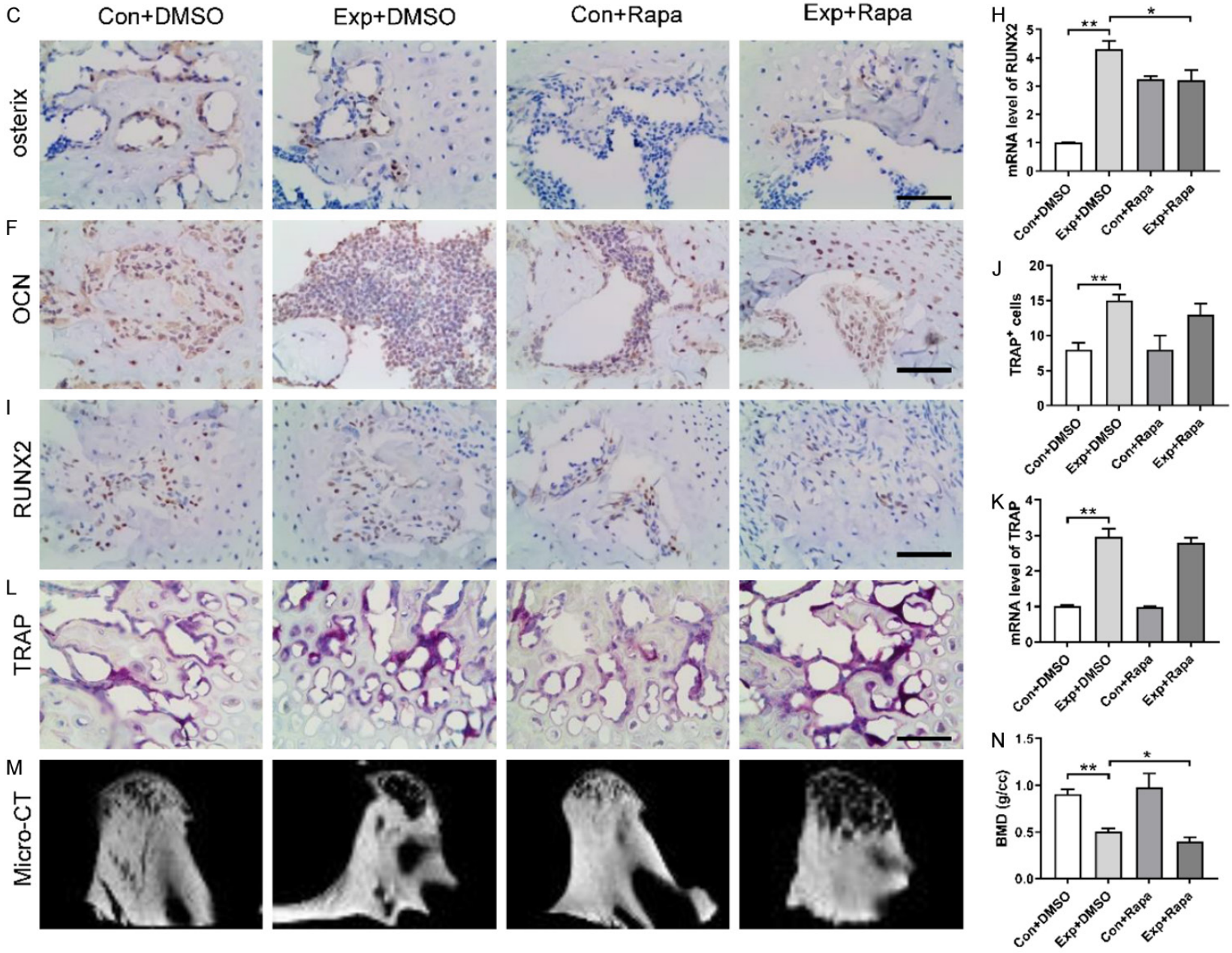
C
Con+DMSO
Exp+DMSO
Con+Rapa
Exp+Rapa
osterix
F
OCN
I
RUNX2
L
TRAP
M
Micro-CT
H
mRNA level of RUNX2
J
TRAP+ cells
K
mRNA level of TRAP
N
BMD (g/cc)

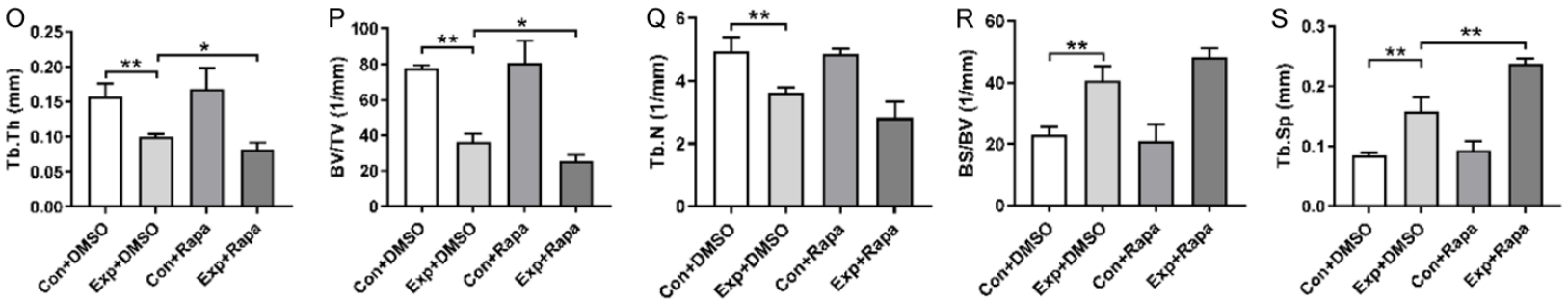

Figure 5. Inhibition of the mTORC1 pathway in the condyle subchondral bone, aggravated subchondral bone loss, and development of TMJ OA. (A-C) Representative quantitative analyses of osterix+ preosteoblasts (A) and mRNA expression levels of osterix (B), and immunohistochemically stained images (C) in the condyle subchondral bone 8 weeks after the procedure in four groups. Scale bars, 50 μm. (D-F) Representative quantitative analyses of OCN+ osteoblasts (D) and mRNA expression levels of OCN (E), and immunohistochemically stained images (F) in the condyle subchondral bone 8 weeks after the procedure in four groups. Scale bars, 50 μm. (G-I) Representative quantitative analyses of RUNX2+ osteoblasts (G) and mRNA expression levels of RUNX2 (H), and immunohistochemically stained images (I) in the condyle subchondral bone 8 weeks after the procedure in four groups. Scale bars, 50 μm. (J-L) Representative quantitative analyses of osteoclasts (J) and mRNA expression levels of TRAP (K), and immunohistochemically stained images (L) in the condyle subchondral bone 8 weeks after the procedure in four groups. Scale bars, 50 μm. (M) Micro-CT images of sagittal sections and quantitative analysis of the condyle subchondral bone 8 weeks after the procedure in four groups. (N-S) Quantitative analyses of bone mass in the subchondral bone. (N) BMD (g/cc), bone mineral density; (O) Tb.N (1/mm), trabecular cell number; (P) Tb.Th (mm), trabecular thickness; (Q) BV/TV (%), bone volume fraction; (R) BS/BV (1/mm), bone surface volume fraction; (S) Tb.Sp (mm), trabecular separation. $*P < 0.05$. $**P < 0.01$.

progression of OA. In addition, current surgical models cannot simulate the natural occurrence and development of human diseases. We have established a rat malocclusion model to make the occurrence of TMJ OA more authentic, thereby better simulating the development of human disease. In our study, only rats between 2 and 8 weeks after the procedure were analyzed. At this time, the Exp group showed decreased cartilage matrix proteoglycan levels, chondrocyte aggregation and hypertrophy, and resorption of the condyle subchondral bone (**Figure 2A** and **2B**). These factors are typical of early TMJ OA [25]. These results above suggested that TMJ OA was successfully established in rats by the overly forward extension of the mandible and that the TMJ was in the early stages of OA.

The early pathological features of TMJ OA are loss of the cartilage matrix and cartilage fibrosis. The late pathological features are cartilage fissures and detachment, with the condyle subchondral bone exhibiting osteosclerosis and osteophyte hyperplasia [26]. Studies on condylar cartilage and subchondral bone show the existence of a close relationship between the articular cartilage and subchondral bone [9, 10]. The basic function of the condyle subchondral bone is to absorb stress and maintain the shape of the joint. In addition, the subchondral bone contains a large number of blood vessels and nerves, and many of their branches enter the calcified cartilage layer to provide nutrition [27]. Compared with the articular cartilage, the subchondral bone is more sensitive to trauma and exhibits more active remodeling. Subchondral bone exhibits an important buffering effect during the process of absorbing abnormal stress [28]. Therefore, when the condyle is subjected to mechanical stress, corresponding changes will occur, such as morphological changes, which will cause subchondral bone remodeling; thus, the shape, arrangement, and density of the subchondral bone trabeculae will also change [29, 30]. In recent years, many researchers have found that the number of bone trabeculae is reduced in the early stages of OA and that the bone density is increased in later stages of OA, which reduces the mechanical properties of the subchondral bone [12]. A separate studied reported that abnormal stresses placed on the condyle could cause microfractures of the subchondral bone, followed by abnormal subchondral bone loss and remodeling, which in turn could lead to subchondral bone sclerosis, cartilage degeneration, and matrix loss [31]. This study confirmed that appliances that overly extend the mandible forward can induce early TMJ OA, with reduced trabecular bone density and number of trabecular bone cells and reduced subchondral bone density.

MTORC1 plays important regulatory roles in cancer, aging, autophagy, and metabolism [32, 33]. A previous study confirmed that mTORC1 is highly expressed in articular cartilage during the progression of OA, which can be affected by the regulation of mTORC1 activation [34]. This process may result from the increased autophagy of chondrocytes or the increased release of inflammatory factors such as TNF-α and IL-1 that are activated by the mTORC1 signaling pathway. The activation of mTORC1 in tibial bone preosteoblasts promotes OA by stimulating bone sclerosis and secretion of CXCL12, but the role of mTORC1 in the reconstruction of subchondral bone during TMJ OA is not clear [22]. This study confirmed that mTORC1 is also highly expressed in the condyle subchondral bone. We observed that changes in the mechanical load on the condyle increase the activity of the mTORC1 signaling pathway. By inhibiting the activation of mTORC1 in osterix+ cells, we inhibited the proliferation of osteoblasts and accelerated subchondral bone loss. These results fully confirm the important regulatory role of mTORC1 in TMJ OA. Although mTORC1 is clearly involved in the differentiation of osteoblasts, it is unclear which downstream effector(s) mediate the function of mTORC1. It will be interesting to determine the downstream mediators of mTORC1 in osteoblast differentiation.

Taken together, the results of this study suggest the regulatory effect of mTORC1 on the condyle subchondral bone during early TMJ OA. We show that mTORC1 produced by preosteoblasts during TMJ OA plays a key role in subchondral bone reconstruction. Abnormal mechanical loading activates mTORC1 in subchondral mandibular condylar preosteoblasts, and inhibition of mTORC1 activation can aggravate subchondral bone loss and accelerate condylar degeneration in the early stages of TMJ OA. Similarly, because of subchondral bone sclerosis in advanced OA, the inhibition of mTORC1 activation may alleviate subchondral bone scle-

rosis and reduce OA progression in advanced OA. Due to the differences between the early and advanced manifestations of OA, staged interference of mTORC1 signaling is an obvious future clinical approach to the treatment of OA. Future studies are warranted to clarify the mechanisms by which the mTORC1 signaling pathway is involved in the regulation of osteoblasts during TMJ OA and the role of the mTORC1 signaling pathway in advanced stages of OA.

Acknowledgements

The present study was supported by the National Natural Science Foundation of China (Grant number: 31870929) and the Natural Science Foundation of Shandong (Grant number: ZR2019MH007).

Disclosure of conflict of interest

None.

Address correspondence to: Drs. Qiang Zhang and Xiao Yuan, Department of Orthodontics, The Affiliated Hospital of Qingdao University, Qingdao 266000, Shandong, China. E-mail: zqzbyzh@163.com (QZ); Tel: +86-0532-82913212; E-mail: yuanxiaoqd@163.com (XY)

References

[1] Wang XD, Zhang JN, Gan YH and Zhou YH. Current understanding of pathogenesis and treatment of TMJ osteoarthritis. J Dent Res 2015; 94: 666-673.

[2] Chen D, Shen J, Zhao W, Wang T, Han L, Hamilton JL and Im HJ. Osteoarthritis: toward a comprehensive understanding of pathological mechanism. Bone Res 2017; 5: 16044.

[3] Liu J, Dai J, Wang Y, Lai S and Wang S. Significance of new blood vessels in the pathogenesis of temporomandibular joint osteoarthritis. Exp Ther Med 2017; 13: 2325-2331.

[4] Tanaka E, Detamore MS and Mercuri LG. Degenerative disorders of the temporomandibular joint: etiology, diagnosis, and treatment. J Dent Res 2008; 87: 296-307.

[5] Kameoka S, Matsumoto K, Kai Y, Yonehara Y, Arai Y and Honda K. Establishment of temporomandibular joint puncture technique in rats using in vivo micro-computed tomography (R_mCT®). Dentomaxillofac Radiol 2010; 39: 441-445.

[6] Krisjane Z, Urtane I, Krumina G, Neimane L and Ragovska I. The prevalence of TMJ osteoarthritis in asymptomatic patients with dentofacial deformities: a cone-beam CT study. Int J Oral Maxillofac Surg 2012; 41: 690-695.

[7] Wang MQ, Xue F, He JJ, Chen JH, Chen CS and Raustia A. Missing posterior teeth and risk of temporomandibular disorders. J Dent Res 2009; 88: 942-945.

[8] Zhang J, Jiao K, Zhang M, Zhou T, Liu XD, Yu SB, Lu L, Jing L, Yang T, Zhang Y, Chen D and Wang MQ. Occlusal effects on longitudinal bone alterations of the temporomandibular joint. J Dent Res 2013; 92: 253-259.

[9] Jiao K, Niu LN, Wang MQ, Dai J, Yu SB, Liu XD and Wang J. Subchondral bone loss following orthodontically induced cartilage degradation in the mandibular condyles of rats. Bone 2011; 48: 362-371.

[10] Arjmand H, Nazemi M, Kontulainen SA, McLennan CE, Hunter DJ, Wilson DR and Johnston JD. Mechanical metrics of the proximal tibia are precise and differentiate osteoarthritic and normal knees: a finite element study. Sci Rep 2018; 8: 11478.

[11] Ketola JH, Karhula SS, Finnilä MAJ, Korhonen RK, Herzog W, Siltanen S, Nieminen MT and Saarakkala S. Iterative and discrete reconstruction in the evaluation of the rabbit model of osteoarthritis. Sci Rep 2018; 8: 12051.

[12] Maruotti N, Corrado A and Cantatore FP. Osteoblast role in osteoarthritis pathogenesis. J Cell Physiol 2017; 232: 2957-2963.

[13] Findlay DM and Atkins GJ. Osteoblast-chondrocyte interactions in osteoarthritis. Curr Osteoporos Rep 2014; 12: 127-134.

[14] Burr DB and Gallant MA. Bone remodelling in osteoarthritis. Nat Rev Rheumatol 2012; 8: 665-673.

[15] Embree M, Ono M, Kilts T, Walker D, Langguth J, Mao J, Bi Y, Barth JL and Young M. Role of subchondral bone during early-stage experimental TMJ osteoarthritis. J Dent Res 2011; 90: 1331-1338.

[16] Yan D, Liu TX, Liu BY, Wang L, Qian ZH, Cheng XG and Li KC. Effects of structural changes in subchondral bone on articular cartilage in a beagle dog model. Biomed Environ Sci 2017; 30: 194-203.

[17] Sun Y, Scannell BP, Honeycutt PR, Mauerhan DR, H JN and Hanley EN Jr. Cartilage degeneration, subchondral mineral and meniscal mineral densities in hartley and strain 13 guinea pigs. Open Rheumatol J 2015; 9: 65-70.

[18] Laplante M and Sabatini DM. mTOR signaling in growth control and disease. Cell 2012; 149: 274-293.

[19] Wullschleger S, Loewith R and Hall MN. TOR signaling in growth and metabolism. Cell 2006; 124: 471-484.

[20] Loewith R and Hall MN. Target of rapamycin (TOR) in nutrient signaling and growth control. Genetics 2011; 189: 1177-1201.

[21] Jacinto E and Hall MN. Tor signalling in bugs, brain and brawn. Nat Rev Mol Cell Biol 2003; 4: 117-126.
[22] Lin C, Liu L, Zeng C, Cui ZK, Chen Y, Lai P, Wang H, Shao Y, Zhang H, Zhang R, Zhao C, Fang H, Cai D and Bai X. Activation of mTORC1 in subchondral bone preosteoblasts promotes osteoarthritis by stimulating bone sclerosis and secretion of CXCL12. Bone Res 2019; 7: 5.
[23] Cohen WA, Servais JM, Polur I, Li Y and Xu L. Articular cartilage degeneration in the contralateral non-surgical temporomandibular joint in mice with a unilateral partial discectomy. J Oral Pathol Med 2014; 43: 162-165.
[24] Long E, Motwani R, Reece D, Pettit N, Hepworth J, Wong P, Reynolds P and Seegmiller R. The role of TGF-ß1 in osteoarthritis of the temporomandibular joint in two genetic mouse models. Arch Oral Biol 2016; 67: 68-73.
[25] Glasson SS, Chambers MG, Van Den Berg WB and Little CB. The OARSI histopathology initiative - recommendations for histological assessments of osteoarthritis in the mouse. Osteoarthritis Cartilage 2010; 18 Suppl 3: S17-23.
[26] Yang T, Zhang J, Cao Y, Zhang M, Jing L, Jiao K, Yu S, Chang W, Chen D and Wang M. Wnt5a/Ror2 mediates temporomandibular joint subchondral bone remodeling. J Dent Res 2015; 94: 803-812.
[27] Riordan EA, Little C and Hunter D. Pathogenesis of post-traumatic OA with a view to intervention. Best Pract Res Clin Rheumatol 2014; 28: 17-30.
[28] Castañeda S, Roman-Blas JA, Largo R and Herrero-Beaumont G. Subchondral bone as a key target for osteoarthritis treatment. Biochem Pharmacol 2012; 83: 315-323.
[29] Fowler TW, Acevedo C, Mazur CM, Hall-Glenn F, Fields AJ, Bale HA, Ritchie RO, Lotz JC, Vail TP and Alliston T. Glucocorticoid suppression of osteocyte perilacunar remodeling is associated with subchondral bone degeneration in osteonecrosis. Sci Rep 2017; 7: 44618.
[30] Lajeunesse D and Reboul P. Subchondral bone in osteoarthritis: a biologic link with articular cartilage leading to abnormal remodeling. Curr Opin Rheumatol 2003; 15: 628-633.
[31] Fazzalari NL, Kuliwaba JS and Forwood MR. Cancellous bone microdamage in the proximal femur: influence of age and osteoarthritis on damage morphology and regional distribution. Bone 2002; 31: 697-702.
[32] Wang L, Pan Y, Huang M, You X, Guo F and Chen Y. PAQR3 augments amino acid deprivation-induced autophagy by inhibiting mTORC1 signaling. Cell Signal 2017; 33: 98-106.
[33] Di Conza G, Trusso Cafarello S, Loroch S, Mennerich D, Deschoemaeker S, Di Matteo M, Ehling M, Gevaert K, Prenen H, Zahedi RP, Sickmann A, Kietzmann T, Moretti F and Mazzone M. The mTOR and PP2A pathways regulate PHD2 phosphorylation to fine-tune HIF1α levels and colorectal cancer cell survival under hypoxia. Cell Rep 2017; 18: 1699-1712.
[34] Zhang H, Wang H, Zeng C, Yan B, Ouyang J, Liu X, Sun Q, Zhao C, Fang H, Pan J, Xie D, Yang J, Zhang T, Bai X and Cai D. mTORC1 activation downregulates FGFR3 and PTH/PTHrP receptor in articular chondrocytes to initiate osteoarthritis. Osteoarthritis Cartilage 2017; 25: 952-963.